

# Journal of Mechanics of Materials and Structures

**AN APPROXIMATE FORMULA OF FIRST PEAK FREQUENCY  
OF ELLIPTICITY OF RAYLEIGH SURFACE WAVES  
IN AN ORTHOTROPIC LAYERED HALF-SPACE MODEL**

Truong Thi Thuy Dung, Tran Thanh Tuan, Pham Chi Vinh and Giang Kien Trung

**Volume 15, No. 1**

**January 2020**





## AN APPROXIMATE FORMULA OF FIRST PEAK FREQUENCY OF ELLIPTICITY OF RAYLEIGH SURFACE WAVES IN AN ORTHOTROPIC LAYERED HALF-SPACE MODEL

TRUONG THI THUY DUNG, TRAN THANH TUAN, PHAM CHI VINH AND GIANG KIEN TRUNG

The propagation of Rayleigh surface waves in an orthotropic composite layer with fixed bottom is considered by using the transfer matrix method. By considering the critical frequency, an explicit approximate formula of the peak frequency of the fundamental mode of H/V ratio curve is derived. In case the impedance contrast between the half-space and the layer is high, the obtained formula is shown to be the limit of the formula of the resonance frequency of the layers under the excitement of SH body waves, which demonstrates that the peak frequency of the H/V ratio could be interpreted as the resonance frequency of the layer. Since Rayleigh surface waves are easier to be excited than SH body incident waves traveling from the half-space to the surface of the layer, and the H/V ratio is a dimensionless quantity and it is easier to be measured than the response function of SH body waves, the obtained formula is potentially useful in measuring the resonance frequency of thin films deposited on a thick layer of substantially higher rigidity. Finally, some numerical calculations are carried out to illustrate that the obtained approximate formula is a good one for the resonance frequency of a composite layer, especially of a periodic composite layer.

### 1. Introduction

In seismology, identifying the resonance frequency of a soft sediment layer is important and meaningful in evaluating the destruction to a city located over the zone of a sediment. Since the traditional methods such as borehole are costly and harmful to the surrounding environment, the H/V ratio technique has been used intensively in recent decades. This method uses the information of peak frequency of the recorded ratio of the horizontal to vertical displacements' amplitude spectra (H/V ratio) at the free surface to deduce the resonance frequency.

From the theoretical point of view and from the fact that the horizontal movement is the main reason to cause the destruction of the structures on the ground, the resonance frequency of the layer should be identified from the first peak of the SH body wave transfer function. This is the function of frequency showing the amplification of the magnitude of an SH body incident wave from the half-space to the surface of the layer. For the simple model of one layer over the half-space, the resonance frequency is [Nakamura 1989]

$$f_r = \frac{1}{4} \frac{\beta}{h}, \quad (1)$$

---

*Keywords:* Rayleigh waves, SH body waves, orthotropy, H/V technique, resonance frequency, transfer matrix.

where  $h$  is the thickness of the layer, and  $\beta$  is the SH wave speed in the layer. This formula is equivalent to

$$\frac{hf_r}{\beta} = \frac{h}{\lambda_\beta} = \frac{1}{4}, \quad (2)$$

where  $\lambda_\beta$  is the wavelength of SH wave at the resonance frequency. Therefore, this formula is called the quarter-wavelength law in determining the resonance frequency, meaning that the thickness of the layer is one quarter of the wavelength of the SH wave propagating at resonance frequency.

In practice, recording the transfer function of SH waves is only feasible in strong or moderate earthquakes in which the SH signal is dominated. But this data is not always available. Thus, the ambient noise is recorded instead. However, the composition of the recorded ambient noise is still controversial since it is believed to be composed of various types of waves such as surface waves, body waves, etc., and the different modes of surface waves other than the fundamental mode could interfere [Lunedei and Malischewsky 2015]. With many investigations based on the recorded data and on the synthetic data, scientists agree that to identify the resonance frequency the recorded ambient noise could be used as the data of the fundamental mode of Rayleigh waves when the impedance contrast of the layer and the half-space is big enough. Therefore, the first peak frequency of the fundamental mode of Rayleigh surface waves could be interpreted as the fundamental resonance frequency of the layer [Field and Jacob 1993; 1995; Lachetl and Bard 1994; Lermo and Chávez-García 1994; Bonnefoy-Claudet et al. 2006].

For a simple isotropic model of one layer over the half-space, the first H/V ratio peak frequency  $f_p$  of the fundamental mode of Rayleigh waves was shown to approach the resonance frequency of the layer  $f_r$  when the impedance contrast increases [Tuan et al. 2011]. For more complex models consisting of many isotropic layers over the half-space, this is also shown in [Tuan et al. 2016a].

In addition to being used in seismology to estimate the resonance frequency of a layer, the H/V ratio technique could be used in material science for orthotropic structures. It is because the H/V ratio is a dimensionless quantity and is easy to be measured [Junge et al. 2006], and Rayleigh waves could be actively excited in thin films over a thick layer structure, that the recorded H/V spectral ratio could contain only Rayleigh waves, not interfered by other waves as in seismology. The question addressed here is whether the orthotropy affects the estimation of the resonance frequency. It is shown in [Vinh et al. 2019] that although the orthotropy considerably affects the H/V ratio behavior, it does not greatly affect the peak frequency of the fundamental mode when the impedance contrast is high. However, this is the case for the model of a single orthotropic layer over a half-space.

This paper aims at proving that the resonance frequency of a stack of layers could be identified from the first peak frequency of the fundamental mode of Rayleigh surface waves not only for isotropic materials but also for orthotropic materials when the impedance contrast of the layers and the half-space is big enough. The paper uses the transfer matrix of an orthotropic layer to establish the dispersion equation and the H/V ratio formula of Rayleigh surface waves propagating in the model of a stack of layers with the bottom fixed and the top surface free. This model is the limiting case of the model layered half-space when the impedance contrast between the half-space and the layer goes to infinity. For the isotropic layer, the transfer matrix was introduced by [Thomson 1950; Haskell 1953] in explicit form, but the explicit form of this matrix for the orthotropic layer has just been given recently in [Vinh et al. 2015; 2016]. Then an explicit equation determining the first peak frequency of H/V ratio as the first singularity of the H/V ratio curve is obtained. Next, an approximate formula of the peak frequency is derived from this explicit

equation given in the form of the quarter-wavelength law. This formula is of the limiting form of the formula of first peak frequency of the SH-wave transfer function in the multilayered half-space model given in [Tuan et al. 2016b] when the impedance contrast goes to a high value. Finally, some numerical results are carried out to illustrate that the obtained approximate formula can estimate the resonance frequency of a composite layer well, especially of a periodic composite layer.

## 2. Rayleigh surface waves in a model of orthotropic multilayers with fixed bottom

**2.1. The dispersion equation.** Consider a composite layer composed of a stack of  $N$  homogeneous orthotropic layers. It is assumed that the  $N$ -th (last) layer has its bottom clamped (fixed) and the first (top) layer has its surface free. The layers are in welded contact and the principal material directions of layers are identical. For layer  $m$  ( $m = 1, \dots, N$ ), and for the problem of plane waves, we denote by  $c_{11}^{(m)}, c_{12}^{(m)}, c_{22}^{(m)}, c_{66}^{(m)}, \rho_m, h_m$  the material parameters in the  $0x_1x_2$  plane (with  $0x_1$  pointing along a principal material direction within the layer and  $0x_2$  along the other principal material direction through the layer), the density of mass, and the thickness of the  $m$ -th layer, respectively. Assume that the Rayleigh waves propagate along the  $x_1$ -direction and decay in the  $x_2$ -direction. The thickness of the composite layer is the total thickness of  $N$  layers and is denoted by  $h = h_1 + h_2 + \dots + h_N$ .

Consider the plane strain problems

$$u_i = u_i(x_1, x_2, t), \quad u_3 \equiv 0, \quad (3)$$

where  $u_i$  ( $i = 1, 2$ ) are displacement components in the  $x_1$ - and  $x_2$ -directions and  $t$  is the time.

For a general orthotropic material, the strain-stress relations of the plane problems are [Ting 1996]

$$\begin{aligned} \sigma_{11} &= c_{11}u_{1,1} + c_{12}u_{2,2}, \\ \sigma_{22} &= c_{12}u_{1,1} + c_{22}u_{2,2}, \\ \sigma_{12} &= c_{66}(u_{1,2} + u_{2,1}), \end{aligned} \quad (4)$$

where  $c_{ij}$  are material constants of the layer.

In the absence of body forces the equations of motion are

$$\begin{aligned} \sigma_{11,1} + \sigma_{12,2} &= \rho \ddot{u}_1, \\ \sigma_{12,1} + \sigma_{22,2} &= \rho \ddot{u}_2, \end{aligned} \quad (5)$$

where  $\sigma_{ij}$  are the stress components, commas indicate differentiation with respect to spatial variable  $x_k$  ( $k = 1, 2$ ), and a dot shows differentiation with respect to the time  $t$ .

If we consider plane waves propagating in the  $x_1$ -direction with apparent velocity  $c$ , apparent wave number  $k$ , and decaying in the  $x_2$ -direction, the displacements and stresses are of forms [Vinh et al. 2016]

$$u_1 = U_1(x_2)e^{ik(x_1-ct)}, \quad u_2 = U_2(x_2)e^{ik(x_1-ct)}, \quad (6)$$

$$\sigma_{12} = k\Sigma_1(x_2)e^{ik(x_1-ct)}, \quad \sigma_{22} = k\Sigma_2(x_2)e^{ik(x_1-ct)}. \quad (7)$$

Consider the layer  $j$  of thickness  $h_j$ ; the transfer matrix which relates the displacement-stress vector  $\xi(x_2) = [U_1 \ U_2 \ \Sigma_1 \ \Sigma_2]^T(x_2)$  at the top ( $x_2 = 0$ ) and at the bottom ( $x_2 = h_j$ ) of the layer is

$$\xi(\text{top}) = \mathbf{T}^{(j)}\xi(\text{bottom}), \quad (8)$$



where matrix  $\mathbf{T}^{(j)}$  is given in [Vinh et al. 2016] as

$$\mathbf{T}^{(j)} = \begin{pmatrix} \mathbf{T}_1^{(j)} & \mathbf{T}_2^{(j)} \\ \mathbf{T}_3^{(j)} & \mathbf{T}_4^{(j)} \end{pmatrix} \quad (9)$$

with the elements given in the Appendix in explicit forms depending on the parameters of the layer, the apparent velocity, and the frequency.

The relation of the displacement-stress vector at the free top surface and at the fixed bottom of the composite layer could be obtained by applying the relation (8) successively for all layers  $j = 1, \dots, N$  in the form

$$\boldsymbol{\xi}(0) = \mathbf{T} \boldsymbol{\xi}(h), \quad (10)$$

where  $\mathbf{T}$  is the global transfer matrix and is the product of all the local matrices of  $N$  layers and is expressed in the form

$$\mathbf{T} = \mathbf{T}^{(N)} \dots \mathbf{T}^{(2)} \mathbf{T}^{(1)}. \quad (11)$$

Due to the traction-free condition at the surface, the displacement-stress vector at the top surface of the composite layer is

$$\boldsymbol{\xi}(0) = [U_1(0) \ U_2(0) \ 0 \ 0]^T. \quad (12)$$

And due to the clamped condition at the bottom, the displacement-stress vector at the fixed bottom of the composite layer is

$$\boldsymbol{\xi}(h) = [0 \ 0 \ \Sigma_1(h) \ \Sigma_2(h)]^T. \quad (13)$$

Substituting these two vectors of displacement-stress into (10), we obtain two equations for the traction-free conditions at  $x_2 = 0$  as

$$\begin{aligned} T_{33}\Sigma_1(h) + T_{34}\Sigma_2(h) &= 0, \\ T_{43}\Sigma_1(h) + T_{44}\Sigma_2(h) &= 0. \end{aligned} \quad (14)$$

The condition for this system of equations having nontrivial solutions is that the determinant of the system of coefficients vanishes. This is the dispersion equation of Rayleigh surface waves which helps determine the phase velocity  $c$  in terms of frequency and it is of form

$$T_{33}T_{44} - T_{34}T_{43} = 0, \quad (15)$$

where  $T_{ij}$  ( $i, j = 3, 4$ ) are the entries ( $i, j$ ) of the global transfer matrix  $\mathbf{T}$ .

The H/V ratio (or ellipticity) of the Rayleigh surface waves is defined as the ratio of the horizontal displacement to the vertical displacement of particles at the free surface of the composite plate and therefore is of form

$$\chi = \frac{U_1(0)}{U_2(0)} = \frac{T_{13}\Sigma_1(h) + T_{14}\Sigma_2(h)}{T_{23}\Sigma_1(h) + T_{24}\Sigma_2(h)}. \quad (16)$$

By using (14) we have

$$\chi = \frac{-T_{13}T_{44} + T_{14}T_{43}}{-T_{23}T_{44} + T_{24}T_{43}}. \quad (17)$$

The asymptotic form of the dispersion equation (15) and the formula of H/V ratio (17) will be expressed in explicit form in terms of the explicit form of the local transfer matrix of an orthotropic layer given in

[Vinh et al. 2016]. The asymptotic form will be used to establish an approximate formula of the peak frequency of H/V ratio curve.

**2.2. The cutoff and singularity frequency equation.** Equation (15) is an implicit equation showing the relation of the phase velocity of Rayleigh waves  $c$  depending on frequency  $f$ . As shown in [Tolstoy and Usdin 1953; Tuan et al. 2016a], the solution of the dispersion equation (15) consists of many modes corresponding to many separate curves of phase velocity  $c$  as a function of frequency  $f$ . Each mode exists if the frequency is greater than a certain value of frequency  $f_c$  which is called the critical frequency or cutoff frequency. At the cutoff frequencies, both the phase velocity  $c$  and the H/V ratio go to infinity. Therefore, to identify the sharp peak (singularity) frequency of the ellipticity of Rayleigh waves of the fundamental mode, we find the cutoff frequency of the fundamental mode by identifying the lowest frequency at which the phase velocity goes to infinity.

The local transfer matrix of the  $m$ -th layer is given in the Appendix. Its elements depend on the parameters of the layer  $m$  and the phase velocity  $c$  and frequency  $f$ . When  $c \rightarrow \infty$ , the asymptotic form of this local transfer matrix, with explanation given in the Appendix, is

$$\mathbf{T}_m = \begin{pmatrix} \cos \bar{\varepsilon}_{2m} & \frac{i c_2^{(m)}}{c} (\alpha_{12}^{(m)} \sin \bar{\varepsilon}_{1m} + \beta_{12}^{(m)} e_3 \sin \bar{\varepsilon}_{2m}) \\ -\frac{i c_2^{(m)}}{c} (\alpha_{21}^{(m)} \sin \bar{\varepsilon}_{1m} - \beta_{21}^{(m)} \sin \bar{\varepsilon}_{2m}) & \cos \bar{\varepsilon}_{1m} \\ \frac{c c_{66}^{(m)}}{c_2^{(m)}} \sin \bar{\varepsilon}_{2m} & i c_{66}^{(m)} \alpha_{32}^{(m)} (\cos \bar{\varepsilon}_{1m} - \cos \bar{\varepsilon}_{2m}) \\ i c_{66}^{(m)} \alpha_{41}^{(m)} (\cos \bar{\varepsilon}_{1m} - \cos \bar{\varepsilon}_{2m}) & \frac{c c_{66}^{(m)}}{c_2^{(m)}} \alpha_{42}^{(m)} \sin \bar{\varepsilon}_{1m} \\ -\frac{c_2^{(m)}}{c c_{66}^{(m)}} \sin \bar{\varepsilon}_{2m} & \frac{i c_2^{(m)2}}{c^2 c_{66}^{(m)}} \alpha_{14}^{(m)} (\cos \bar{\varepsilon}_{1m} - \cos \bar{\varepsilon}_{2m}) \\ -\frac{i c_2^{(m)2}}{c^2 c_{66}^{(m)}} \alpha_{23}^{(m)} (\cos \bar{\varepsilon}_{1m} - \cos \bar{\varepsilon}_{2m}) & -\frac{c_2^{(m)}}{c c_{66}^{(m)}} \alpha_{24}^{(m)} \sin \bar{\varepsilon}_{1m} \\ \cos \bar{\varepsilon}_{2m} & -\frac{i c_2^{(m)}}{c} (\alpha_{34}^{(m)} \sin \bar{\varepsilon}_{1m} + \beta_{34}^{(m)} \sin \bar{\varepsilon}_{2m}) \\ -\frac{i c_2^{(m)}}{c} (\alpha_{43}^{(m)} \sin \bar{\varepsilon}_{1m} - \beta_{43}^{(m)} \sin \bar{\varepsilon}_{2m}) & \cos \bar{\varepsilon}_{1m} \end{pmatrix}, \quad (18)$$

in which each element is expressed as the dominant term in  $c$ . The  $\alpha_{ij}^{(m)}$ ,  $\beta_{ij}^{(m)}$ , and  $\bar{\varepsilon}_{im}$  are given in the Appendix.

From the form of global transfer matrix given in (11), it is straightforward to prove that the global transfer matrix has a similar asymptotic form as the local transfer matrix where the elements  $T_{11}$ ,  $T_{22}$ ,  $T_{33}$ ,  $T_{44}$ ,  $T_{32}$ ,  $T_{41}$  are finite terms (do not depend on  $c$ ), the elements  $T_{21}$ ,  $T_{12}$ ,  $T_{13}$ ,  $T_{24}$ ,  $T_{34}$ ,  $T_{43}$  are of degree  $1/c$ , the elements  $T_{31}$ ,  $T_{42}$  are of degree  $c$ , and the elements  $T_{14}$ ,  $T_{23}$  are of degree  $1/c^2$ . Therefore, when  $c \rightarrow \infty$ , the dispersion equation becomes

$$T_{33} T_{44} = 0 \quad (19)$$

since the term  $T_{34}T_{43}$  is of degree of  $1/c^2$  and is eliminated. This equation is now used to determine the cutoff frequencies which are also the singularity frequencies.

*Simple model of one layer.* In the case of a simple model with one layer only, the global transfer matrix is the local transfer matrix of that layer and is of the form (18). In this case, the cutoff frequency equation of Rayleigh waves is

$$T_{33}T_{44} = \cos \bar{\varepsilon}_2 \cos \bar{\varepsilon}_1 = 0. \quad (20)$$

The solutions of  $T_{33} = \cos \bar{\varepsilon}_2 = 0$  are

$$\frac{fh}{c_2} = \frac{1}{4} + \frac{n}{2}, \quad n = 0, 1, 2, \dots, \quad (21)$$

where  $c_2 = \sqrt{c_{66}/\rho}$  is the velocity of an SH-type wave propagating in the layer. These solutions are the cutoff frequencies of symmetric modes as classified in [Tolstoy and Usdin 1953]. The solutions of  $T_{44} = \cos \bar{\varepsilon}_1 = 0$  are

$$\frac{fh}{c_2\sqrt{e_2}} = \frac{1}{4} + \frac{l}{2}, \quad l = 0, 1, 2, \dots, \quad (22)$$

which are cutoff frequencies of asymmetric modes. Since  $e_2 = c_{22}/c_{66} > 1$ , the cutoff frequency of the fundamental mode belongs to the solution class of symmetric modes with  $n = 0$  in (21). This solution corresponds to the quarter-wavelength law for the isotropic models stated in (1)–(2). The other cutoff frequencies of the asymmetric modes and symmetric modes are of the higher modes.

We can see from the asymptotic form of the transfer matrix in (18) that the H/V ratio given by (17) has the asymptotic form proportional to  $c$ . Hence, it goes to infinity as  $c \rightarrow \infty$ . Therefore, the singularity of the H/V ratio of the model layer with bottom fixed is at the cutoff frequency.

*The case of many layers.* If the composite layer is composed of  $N$  different layers, the element  $T_{33}$  of the global transfer matrix is computed from the product in (11) by the recursive equations

$$\begin{aligned} T_{33}^{(n+1)} &= \cos \bar{\varepsilon}_{2(n+1)} T_{33}^{(n)} - \frac{c_2^{(n+1)}}{cc_{66}^{(n+1)}} \sin \bar{\varepsilon}_{2(n+1)} T_{31}^{(n)}, \\ T_{31}^{(n+1)} &= \frac{cc_{66}^{(n+1)}}{c_2^{(n+1)}} \sin \bar{\varepsilon}_{2(n+1)} T_{33}^{(n)} + \cos \bar{\varepsilon}_{2(n+1)} T_{31}^{(n)}, \end{aligned} \quad (23)$$

where  $n$  runs from 1 to  $N - 1$ . The matrix form of this system of equations is

$$\begin{pmatrix} T_{33}^{(n+1)} \\ T_{31}^{(n+1)} \end{pmatrix} = \begin{pmatrix} \cos \bar{\varepsilon}_{2(n+1)} & -\frac{c_2^{(n+1)}}{cc_{66}^{(n+1)}} \sin \bar{\varepsilon}_{2(n+1)} \\ \frac{cc_{66}^{(n+1)}}{c_2^{(n+1)}} \sin \bar{\varepsilon}_{2(n+1)} & \cos \bar{\varepsilon}_{2(n+1)} \end{pmatrix} \times \begin{pmatrix} T_{33}^{(n)} \\ T_{31}^{(n)} \end{pmatrix}. \quad (24)$$

This recursive equation has the same form as the recursive equation for the isotropic models given in (18) in [Tuan et al. 2016a] in which  $c_{66}$  and  $c_2$  are replaced by shear modulus  $\mu$  and shear wave speed  $\beta$ , respectively. Therefore, using the same steps carried out in [Tuan et al. 2016a] we obtain the equation



determining the cutoff frequencies of the orthotropic models as

$$1 + \sum_{j=1}^{\infty} (-1)^j I_j (2\pi f)^{2j} = 1 - I_1 (2\pi f)^2 + I_2 (2\pi f)^4 - \dots = 0, \quad (25)$$

which is in the same form as (27) with coefficients  $I_j$  given in (28) in [Tuan et al. 2016a], in which  $\beta_i$  is replaced by  $c_2^{(i)}$ .

For the composite layer, the approximate equation of (25) is obtained in the same manner as in [Tuan et al. 2016a] and has the form

$$1 - I_1 (2\pi f)^2 = 0, \quad (26)$$

where  $I_1$  is

$$I_1 = \sum_{i=1}^{N-1} \sum_{j=i+1}^N \frac{\rho_i}{\rho_j c_2^{(j)2}} h_i h_j + \frac{1}{2} \sum_{i=1}^N \frac{h_i^2}{c_2^{(j)2}}, \quad (27)$$

where  $c_2^{(j)} = \sqrt{c_{66}^{(j)} / \rho_j}$  is the velocity of SH-type waves in orthotropic layer  $j$ .

Since the recursive equation determining the asymptote global transfer matrix (24) is in a similar form as that of the isotropic case, and in order to get the similar form of the quarter-wavelength law, we define the average shear-wave velocity of the composite layer in the same wave for the isotropic case [Tuan et al. 2016a] as

$$\bar{V} = \frac{h}{\sqrt{2 \sum_{i=1}^{N-1} \sum_{j=i+1}^N (\rho_i / \rho_j c_2^{(j)2}) h_i h_j + \sum_{i=1}^N (h_i^2 / c_2^{(j)2})}}. \quad (28)$$

Then, the solution of the approximate equation (26) is

$$f_p = \frac{1}{4} \frac{\bar{V}}{h}. \quad (29)$$

In dimensionless form, the obtained approximate formula of the first peak of H/V ratio of Rayleigh surface waves in layered half-space is

$$\bar{f}_p = \frac{h f_p}{\bar{V}} = \frac{1}{4}. \quad (30)$$

Note that a factor of  $2\sqrt{2}/\pi$  has been removed with the same argument due to the error of the approximation process given in [Tuan et al. 2016b]. In that paper, the dimensionless resonance frequency of the orthotropic composite layer is given as

$$\bar{f}_r = \frac{h f_r}{\bar{V}} = \frac{1}{4} \sqrt{1 - \frac{I_{(N)}^2}{I_{(HS)}^2}}, \quad (31)$$

where  $I_{(N)}$  and  $I_{(HS)}$  are the impedance values of the composite layer and the half-space defined as

$$I_{(N)} = \bar{\rho} \bar{V}, \quad I_{(HS)} = \rho^{(HS)} c_2^{(HS)}, \quad (32)$$

in which  $\bar{\rho} = (1/h) \sum_{i=1}^N \rho_i h_i$  is the average density of mass of the composite layer and  $\rho^{(HS)}$  and  $c_2^{(HS)}$  are the density of mass and the SH-type wave velocity of the half-space. We can see that while (30) is

obtained from the problem of the Rayleigh surface wave, (31) is the result of the problem of SH body waves. Although the two formulas are derived from different approaches, they are of the same form. The only difference is the factor  $\sqrt{1 - I_{(N)}^2/I_{(HS)}^2}$ . This factor goes to 1 when the impedance value of the half-space is much more than impedance value of the composite layer. That means the resonance frequency  $f_r$  of the layer in (31) tends to the peak frequency of H/V ratio curve  $f_p$  in (30) when the impedance contrast between the half-space and the layer is big enough and we can therefore approximate the peak frequency of the H/V ratio of the recorded noise for the resonance frequency of the orthotropic layer.

### 3. Illustrative examples

This section is to numerically show that the first peak frequency of the H/V ratio of Rayleigh waves can be interpreted as the fundamental resonance frequency of a composite layer over a rigid half-space when the impedance contrast between the layer and the half-space is large enough. This has practical meaning since a Rayleigh surface wave propagating on the surface of the composite layer is easier to be excited and measured than an SH body wave traveling from within the half-space to the surface of the layer. The first part of this section is for a composite layer made from two orthotropic layers. The second part is for a periodic composite layer consisting of many unit cells made of the same two orthotropic layers as in the first part.

**3.1. Composite layer.** Consider a model of two orthotropic layers deposited on a half-space. The two layers are made of beryl rock and layered soil (called a composite layer) which are assumed to be of the same thickness. The half-space is assumed to be isotropic. The material constants of this model are given in Table 1, which are extracted from [Wang and Rajapakse 1994, Table 1].

The average shear velocity of the two layers is computed by (28) as  $\bar{V} = 0.7977$  (km/s), while the SH-type wave velocity of the half-space is  $c_2^{(HS)} = \sqrt{c_{66}^{(HS)}/\rho^{(HS)}} = 2$ . Therefore, the impedance contrast between the half-space and the layers of this model computed from (32) is about 2.5. The exact H/V ratio curve of Rayleigh waves depending on frequency is computed numerically by a modified program for orthotropic layered half-space models given in [Tuan and Trung 2016]. The value 2.5 of impedance contrast is classified as low in [Bonnefoy-Claudet et al. 2006]. Therefore, the H/V ratio curve of this model only shows a broad peak at the dimensionless frequency  $\bar{f}_p = 0.2248$  where  $\bar{f}_p$  is defined in (30). The exact fundamental dimensionless resonance frequency of the composite layer computed by the explicit formula given in [Tuan et al. 2016b] is  $\bar{f}_r = 0.2558$ . The obtained approximate formula for the dimensionless resonance frequency always gives the value 0.25 due to the way it is expressed. We can see that in this low-impedance-contrast case, the peak frequency  $\bar{f}_p$  is rather far from 0.25 but the resonance frequency  $\bar{f}_r$  is close to 0.25 with a relative error of 2.3%. It indicates that the obtained approximate formula estimates the exact resonance frequency well.

material	$c_{11}$	$c_{22}$	$c_{12}$	$c_{66}$	$\rho$ (g/cm <sup>3</sup> )
beryl rock	4.13	3.62	1.01	1.0	2
layered soil	6.25	4.57	1.74	1.40	2
half-space	24	24	8	8	2

**Table 1.** Material constants ( $\times 10^9$  N/m<sup>2</sup>).

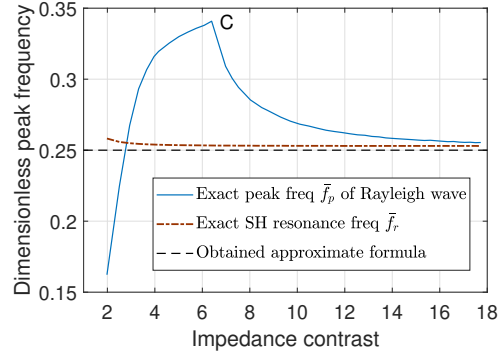


**Figure 1.** The exact peak frequency of H/V ratio curve and the resonance frequency of the composite layer of the orthotropic layered half-space given in Table 1.

To examine the obtained formula, we let the rigidity of the half-space (i.e.,  $c_{66}^{(HS)}$ ) vary such that the impedance contrast between the half-space and the composite layer varies from about 2 to 18, which spans from the low range to the high range of impedance contrast. By this variation of impedance contrast, we examine the change of the first peak frequency of ellipticity of Rayleigh surface waves and the change of resonance frequency and compare them to the obtained approximate formula. Figure 1 shows the change of the dimensionless peak frequency of the model with the above change of impedance contrast. In this figure, the continuous line is the exact peak frequency of the H/V ratio of Rayleigh waves and the dash-dotted line is the exact resonance frequency. By expressing the peak frequency in the dimensionless form (30), the obtained formula always gives  $\bar{f}_p = \frac{1}{4}$ , which is represented by a horizontal dashed line.

We can see from Figure 1 that the exact value of resonance frequency is always between the exact peak frequency of the H/V ratio of Rayleigh waves and the value of the obtained approximate formula. The obtained approximate formula is derived from the Rayleigh surface waves problem and it only approximates the peak frequency of H/V ratio well for high value of impedance contrast. However, it provides a good approximation of the resonance frequency in the whole impedance contrast range. For low impedance contrast, the H/V curves only show a broad peak frequency and its value can be far from the value of the quarter-wavelength law (the first part of the continuous line). When the impedance contrast is big enough, which is greater than a critical value (about 6 for this model and denoted by point  $C$  in the figure), the H/V ratio curves show a sharp peak (singularity point). The point  $C$  has already been reported in [Malischewsky and Scherbaum 2004]. The sharp peak frequency approaches the resonance frequency, which in turns approaches the value given by the quarter-wavelength law when the impedance contrast goes large. In this case, the peak frequency of the H/V ratio curve can therefore be interpreted as the resonance frequency of the layers.

**3.2. Periodic composite layer.** We consider now a composite layer with a periodical structure of  $n$  cells. Each cell is made of two orthotropic layers given in Table 1. The half-space is the same one given in Table 1. As shown in [Tuan et al. 2016b], the average shear velocity of the layers depends strongly on the position of the layer. If this average is taken in a traditional way such as the harmonic mean, the average value is constant despite the number of cells. However, the average formula given in (28) shows the different average value as it should be since the H/V ratio curve of the new model (with more layers)

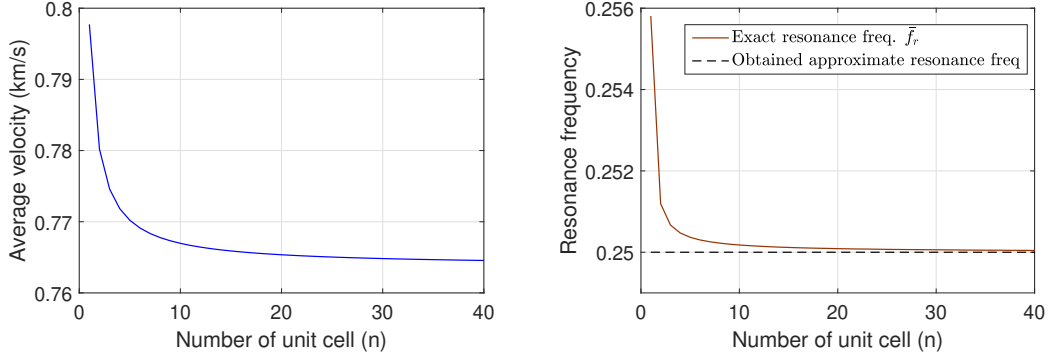


**Figure 2.** The average shear velocity (left) and the exact and approximate dimensionless resonance frequency (right) of the periodic composite layer depending on the number of cells  $n$ .

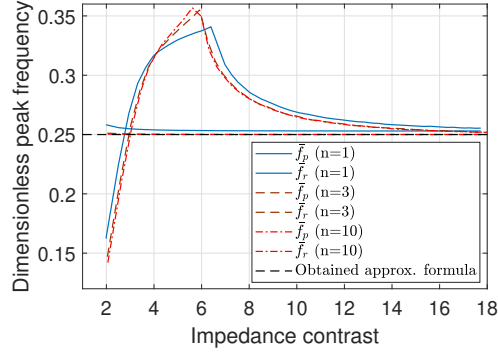


**Figure 3.** The exact peak frequency of the H/V ratio curve and the exact resonance frequency of the periodic composite layer.

should be different from the H/V ratio curve of the original model. This fact is illustrated in Figure 2, left, showing the value of average shear velocity of the periodic composite layer depending on the number of cells  $n$ . When the number  $n$  increases to about 40, the average value tends to a steady value of about 0.7641 (km/s).

Figure 2, right, shows the exact dimensionless resonance frequency of the periodic composite layer depending on the number of cells. When the composite layer has only a single cell, the exact dimensionless resonance frequency is  $\bar{f}_r = 0.2558$  as mentioned above. When the number of cells is  $n = 3$ , that frequency is 0.2507, and when  $n = 10$  it is 0.2502, which is almost equal to the prediction from the obtained approximate formula  $\bar{f}_r = 0.25$ . From this figure, we can see that the obtained approximate formula is substantially good for the periodic structure even for this model of low impedance contrast.

Figure 3 shows similar curves as in Figure 1 but for models of periodic composite layer deposited on the half-space. In this figure, we consider two more models of periodic composite layer with the number of cells  $n = 3$  and  $n = 10$ . The total thicknesses of the layers of the three models are different, but note that the peak and resonance frequencies are given in dimensionless form. We can see that the shapes of the peak frequency curves of the three models are similar and close to each other's despite the considered

number of layers. When the number of cells is greater than 3, the shapes of the exact peak frequency curves of H/V ratios of Rayleigh waves are almost identical and the exact resonance frequency curves almost coincide with the approximate resonance frequency curves. That means the obtained formula is very good for the periodic structure.

#### 4. Conclusions

An explicit approximate formula of the first peak frequency of the H/V ratio curve for the model of a stack of orthotropic layers underlain by a half-space has been derived using the transfer matrix method with the assumption that the impedance contrast between the half-space and the layers is high. It is shown that the obtained formula is the limiting result of the first peak frequency of the transfer function of SH body waves propagating from the half-space. This peak frequency is considered as the resonance frequency of the composite layer. Therefore, the paper has shown for the orthotropic models that when the impedance contrast between the half-space and the layers is high enough, the first peak frequency of the H/V ratio of the Rayleigh surface waves (the singularity) could be used to identify the first peak frequency of the transfer function of SH body waves (the resonance frequency). Although the approximate formula is obtained with the assumption of high impedance contrast between the composite layer and the half-space, it is numerically shown to be a good approximation of the resonance frequency of the composite layer even for moderate values of impedance contrast, especially in the case of periodic composite layer. Since orthotropic materials are widely used in the field of material and the data of Rayleigh surface waves is easier to be measured than the data of SH body waves, the obtained formula is potentially useful in determining the resonance frequency of orthotropic thin films deposited on a hard thick layer.

#### Appendix: Entries of matrix $T_m$

The components of the transfer matrix  $T_m$  of the layer are given in [Vinh et al. 2016] as

$$T_m = \begin{pmatrix} \frac{[\gamma_m; \cosh \varepsilon_m]}{[\gamma_m]} & \frac{-i[\beta_m; \sinh \varepsilon_m]}{[\alpha_m; \beta_m]} & \frac{-[\alpha_m; \sinh \varepsilon_m]}{[\alpha_m; \beta_m]} & \frac{-i[\cosh \varepsilon_m]}{[\gamma_m]} \\ \frac{-i[\gamma_m; \alpha_m \sinh \varepsilon_m]}{[\gamma_m]} & \frac{-ic[\alpha_m \cosh \varepsilon_m; \beta_m]}{[\alpha_m; \beta_m]} & \frac{-i\alpha_{1m}\alpha_{2m}[\cosh \varepsilon_m]}{[\alpha_m; \beta_m]} & \frac{-[\alpha_m \sinh \varepsilon_m]}{[\gamma_m]} \\ \frac{-[\gamma_m; \beta_m \sinh \varepsilon_m]}{[\gamma_m]} & \frac{-i\beta_{1m}\beta_{2m}[\cosh \varepsilon_m]}{[\alpha; \beta]} & \frac{[\gamma_m; \cosh \varepsilon_m]}{[\gamma_m]} & \frac{i[\beta_m \sinh \varepsilon_m]}{[\gamma_m]} \\ \frac{-i\gamma_{1m}\gamma_{2m}[\cosh \varepsilon_m]}{[\gamma_m]} & \frac{-[\beta_m; \gamma_m \sinh \varepsilon_m]}{[\alpha_m; \beta_m]} & \frac{-i[\alpha_m; \gamma_m \sinh \varepsilon_m]}{[\alpha_m; \beta_m]} & \frac{[\gamma_m \cosh \varepsilon_m]}{[\gamma_m]} \end{pmatrix}. \quad (33)$$

In this matrix, we use the notations

$$[f; g] := f_2g_1 - f_1g_2, \quad [f] = f_2 - f_1. \quad (34)$$

The other notations depend on the parameters of the layers  $c_{ij}^{(m)}$ ,  $\rho_m$ ,  $h_m$ , the phase velocity  $c$ , and the wave number  $k$  as

$$\begin{aligned}
\alpha_i^{(m)} &= -\frac{(e_3^{(m)} + 1)b_i^{(m)}}{e_2^{(m)}b_i^{(m)2} - 1 + x_m}, \quad i = 1, 2, & x_m &= \frac{\rho_m c^2}{c_{66}^{(m)}}, \\
b_1^{(m)} &= \sqrt{\frac{S^{(m)} + \sqrt{S^{(m)2} - 4P^{(m)}}}{2}}, & b_2^{(m)} &= \sqrt{\frac{S^{(m)} - \sqrt{S^{(m)2} - 4P^{(m)}}}{2}}, \\
S^{(m)} &= \frac{e_2^{(m)}(e_1^{(m)} - x_m) + 1 - x_m - (e_3^{(m)} + 1)^2}{e_2^{(m)}}, & P^{(m)} &= \frac{(e_1^{(m)} - x_m)(1 - x_m)}{e_2^{(m)}}, \\
\beta_i^{(m)} &= c_{66}^{(m)}(b_i^{(m)} - \alpha_i^{(m)}), & \gamma_i^{(m)} &= e_3^{(m)} + e_2^{(m)}b_i^{(m)}\alpha_i^{(m)}, \\
\varepsilon_{1m} &= b_1^{(m)}kh_m, & \varepsilon_{2m} &= b_2^{(m)}kh_m,
\end{aligned} \tag{35}$$

in which the dimensionless parameters  $e_i^{(m)}$  are defined as

$$e_1^{(m)} = \frac{c_{11}^{(m)}}{c_{66}^{(m)}}, \quad e_2^{(m)} = \frac{c_{22}^{(m)}}{c_{66}^{(m)}}, \quad e_3^{(m)} = \frac{c_{12}^{(m)}}{c_{66}^{(m)}}.$$

For example, we have  $[\cosh \varepsilon_m] = \cosh \varepsilon_{2m} - \cosh \varepsilon_{1m}$ ,  $[\gamma_m; \cosh \varepsilon_m] = \gamma_2^{(m)} \cosh \varepsilon_{1m} - \gamma_1^{(m)} \cosh \varepsilon_{2m}$ , and  $[\alpha_m \sinh \varepsilon_m] = \alpha_2^{(m)} \sinh \varepsilon_{2m} - \alpha_1^{(m)} \sinh \varepsilon_{1m}$ .

When  $c \rightarrow \infty$ , the asymptotic values of  $\varepsilon_{1m}$  and  $\varepsilon_{2m}$  are

$$\varepsilon_{1m} \sim \frac{i2\pi fh_m}{c_2^{(m)} \sqrt{e_2^{(m)}}} := i\bar{\varepsilon}_{1m}, \quad \varepsilon_{2m} \sim \frac{i2\pi fh_m}{c_2^{(m)}} := i\bar{\varepsilon}_{2m}. \tag{36}$$

Since  $\cosh(ix) = \cos(x)$  and  $\sinh(ix) = i \sin(x)$ , the asymptotic values of elements of the transfer matrix  $T_m$  in (33) are

$$\begin{aligned}
(T_m)_{11} &\sim \cos \bar{\varepsilon}_{2m}, & (T_m)_{21} &\sim -\frac{ic_2^{(m)}}{c}(\alpha_{21}^{(m)} \sin \bar{\varepsilon}_{1m} - \beta_{21}^{(m)} \sin \bar{\varepsilon}_{2m}), \\
(T_m)_{12} &\sim \frac{ic_2^{(m)}}{c}(\alpha_{12}^{(m)} \sin \bar{\varepsilon}_{1m} + \beta_{12}^{(m)} e_{3m} \sin \bar{\varepsilon}_{2m}), & (T_m)_{22} &\sim \cos \bar{\varepsilon}_{1m}, \\
(T_m)_{13} &\sim \frac{-cc_{66}^{(m)}}{c_2^{(m)}} \sin \bar{\varepsilon}_{2m}, & (T_m)_{23} &\sim -\frac{ic_2^{(m)2}}{c_2^2 c_{66}^{(m)}} \alpha_{23} (\cos \bar{\varepsilon}_{1m} - \cos \bar{\varepsilon}_{2m}), \\
(T_m)_{14} &\sim \frac{ic_2^{(m)2}}{c_2^2 c_{66}^{(m)}} \alpha_{14} (\cos \bar{\varepsilon}_{1m} - \cos \bar{\varepsilon}_{2m}), & (T_m)_{24} &\sim \frac{-c_2^{(m)}}{cc_{66}^{(m)}} \alpha_{24} \sin \bar{\varepsilon}_{1m}, \\
(T_m)_{31} &\sim \frac{cc_{66}^{(m)}}{c_2^{(m)}} \sin \bar{\varepsilon}_{2m}, & (T_m)_{32} &\sim ic_{66}^{(m)} \alpha_{32}^{(m)} (\cos \bar{\varepsilon}_{1m} - \cos \bar{\varepsilon}_{2m}), \\
(T_m)_{33} &= (T_m)_{11}, & (T_m)_{34} &\sim -\frac{ic_2^{(m)}}{c}(\alpha_{34}^{(m)} \sin \bar{\varepsilon}_{1m} + \beta_{34}^{(m)} \sin \bar{\varepsilon}_{2m}), \\
(T_m)_{41} &\sim ic_{66}^{(m)} \alpha_{41}^{(m)} (\cos \bar{\varepsilon}_{1m} - \cos \bar{\varepsilon}_{2m}), & (T_m)_{42} &\sim \frac{cc_{66}^{(m)}}{c_2^{(m)}} \alpha_{42}^{(m)} \sin \bar{\varepsilon}_{1m}, \\
(T_m)_{43} &\sim -\frac{ic_2^{(m)}}{c}(\alpha_{43}^{(m)} \sin \bar{\varepsilon}_{1m} - \beta_{43}^{(m)} \sin \bar{\varepsilon}_{2m}), & (T_m)_{44} &= (T_m)_{22}
\end{aligned}$$

with

$$\begin{aligned}
 \alpha_{12}^{(m)} &= -\frac{\sqrt{e_2^{(m)}}}{1+e_3^{(m)}}, & \beta_{12}^{(m)} &= -\alpha_{32}^{(m)} = -\frac{e_3^{(m)}}{1+e_3^{(m)}}, & \alpha_{14}^{(m)} &= \beta_{34}^{(m)} = \frac{1}{1+e_3^{(m)}}, \\
 \alpha_{21}^{(m)} &= \frac{e_2^{(m)} + e_3^{(m)}}{\sqrt{e_2^{(m)}}(e_2^{(m)} - 1)}, & \beta_{21}^{(m)} &= \alpha_{23}^{(m)} = \frac{1+e_3^{(m)}}{e_2^{(m)} - 1}, & \alpha_{24}^{(m)} &= \frac{1}{\sqrt{e_2^{(m)}}}, \\
 & & \alpha_{34}^{(m)} &= \frac{e_3^{(m)}}{\sqrt{e_2^{(m)}}(1+e_3^{(m)})}, & & \\
 \alpha_{41}^{(m)} &= \beta_{43}^{(m)} = \frac{e_2^{(m)} + e_3^{(m)}}{e_2^{(m)} - 1}, & \alpha_{42}^{(m)} &= \sqrt{e_2^{(m)}}, & \alpha_{43}^{(m)} &= \frac{\sqrt{e_2^{(m)}}(1+e_3^{(m)})}{e_2^{(m)} - 1}.
 \end{aligned}$$

### Acknowledgments

This research is funded by Vietnam National Foundation for Science and Technology Development (NAFOSTED) under grant number 107.02–2019.06.

### References

- [Bonnefoy-Claudet et al. 2006] S. Bonnefoy-Claudet, F. Cotton, P.-Y. Bard, M. Cornou, C. Ohrnberger, and M. Wathelet, “Robustness of the H/V ratio peak frequency to estimate 1D resonance frequency”, pp. 361–370 in *Third International Symposium on the Effects of Surface Geology on Seismic Motion* (Grenoble, 2006), edited by P.-Y. Bard et al., Laboratoire Central des Ponts et Chaussées, Paris, 2006.
- [Field and Jacob 1993] E. Field and K. Jacob, “The theoretical response of sedimentary layers to ambient seismic noise”, *Geophys. Res. Lett.* **20**:24 (1993), 2925–2928.
- [Field and Jacob 1995] E. H. Field and K. H. Jacob, “A comparison and test of various site-response estimation techniques, including three that are not reference-site dependent”, *B. Seismol. Soc. Am.* **85**:4 (1995), 1127–1143.
- [Haskell 1953] N. A. Haskell, “The dispersion of surface waves on multi-layered media”, *B. Seismol. Soc. Am.* **43** (1953), 17–34.
- [Junge et al. 2006] M. Junge, J. Qu, and L. J. Jacobs, “Relationship between Rayleigh wave polarization and state of stress”, *Ultrasonics* **44**:3 (2006), 233–237.
- [Lachetl and Bard 1994] C. Lachetl and P.-Y. Bard, “Numerical and theoretical investigations on the possibilities and limitations of Nakamura’s technique”, *J. Phys. Earth* **42**:5 (1994), 377–397.
- [Lermo and Chávez-García 1994] J. Lermo and F. J. Chávez-García, “Are microtremors useful in site response evaluation?”, *B. Seismol. Soc. Am.* **84**:5 (1994), 1350–1364.
- [Lunedei and Malischewsky 2015] E. Lunedei and P. Malischewsky, “A review and some new issues on the theory of the H/V technique for ambient vibrations”, pp. 371–394 in *Perspectives on European earthquake engineering and seismology*, vol. 2, edited by A. Ansal, Geotechnical, Geological and Earthquake Engineering **39**, Springer, 2015.
- [Malischewsky and Scherbaum 2004] P. G. Malischewsky and F. Scherbaum, “Love’s formula and H/V-ratio (ellipticity) of Rayleigh waves”, *Wave Motion* **40**:1 (2004), 57–67.
- [Nakamura 1989] Y. Nakamura, “Method for dynamic characteristics estimation of subsurface using microtremor on the ground surface”, *Q. Report RTRI* **30**:1 (1989), 25–33.
- [Thomson 1950] W. T. Thomson, “Transmission of elastic waves through a stratified solid medium”, *J. Appl. Phys.* **21** (1950), 89–93.



- [Ting 1996] T. C. T. Ting, *Anisotropic elasticity: theory and applications*, Oxford Engineering Science Series **45**, Oxford University, 1996.
- [Tolstoy and Usdin 1953] I. Tolstoy and E. Usdin, “Dispersive properties of stratified elastic and liquid media: A ray theory”, *Geophysics* **18** (1953), 844–870.
- [Tuan and Trung 2016] T. T. Tuan and T. N. Trung, “The dispersion of Rayleigh waves in orthotropic layered half-space using matrix method”, *Vietnam J. Mech.* **38**:1 (2016), 27–38.
- [Tuan et al. 2011] T. T. Tuan, F. Scherbaum, and P. G. Malischewsky, “On the relationship of peaks and troughs of the ellipticity (H/V) of Rayleigh waves and the transmission response of single layer over half-space models”, *Geophys. J. Int.* **184**:2 (2011), 793–800.
- [Tuan et al. 2016a] T. T. Tuan, P. C. Vinh, P. Malischewsky, and A. Aoudia, “Approximate formula of peak frequency of H/V ratio curve in multilayered model and its use in H/V ratio technique”, *Pure Appl. Geophys.* **173**:2 (2016), 487–498.
- [Tuan et al. 2016b] T. T. Tuan, P. C. Vinh, M. Ohrnberger, P. Malischewsky, and A. Aoudia, “An improved formula of fundamental resonance frequency of a layered half-space model used in H/V ratio technique”, *Pure Appl. Geophys.* **173**:8 (2016), 2803–2812.
- [Vinh et al. 2015] P. C. Vinh, N. T. K. Linh, and V. T. N. Anh, “On a technique for deriving explicit transfer matrices of orthotropic layers”, *Vietnam J. Mech.* **37**:4 (2015), 303–315.
- [Vinh et al. 2016] P. C. Vinh, V. T. N. Anh, and N. T. K. Linh, “On a technique for deriving the explicit secular equation of Rayleigh waves in an orthotropic half-space coated by an orthotropic layer”, *Waves Random Complex Media* **26**:2 (2016), 176–188.
- [Vinh et al. 2019] P. C. Vinh, T. T. Tuan, L. T. Hue, V. T. N. Anh, T. T. T. Dung, N. T. K. Linh, and P. Malischewsky, “Exact formula for the horizontal-to-vertical displacement ratio of Rayleigh waves in layered orthotropic half-spaces”, *J. Acoust. Soc. Am.* **146**:2 (2019), 1279–1289.
- [Wang and Rajapakse 1994] Y. Wang and R. K. N. D. Rajapakse, “An exact stiffness method for elastodynamics of a layered orthotropic half-plane”, *J. Appl. Mech.* **61**:2 (1994), 339–348.

Received 23 May 2019. Revised 27 Dec 2019. Accepted 29 Jan 2020.

TRUONG THI THUY DUNG: [dungttt@hus.edu.vn](mailto:dungttt@hus.edu.vn)

*Faculty of Mathematics, Mechanics and Informatics, VNU University of Science, Vietnam, Hanoi, Vietnam*

TRAN THANH TUAN: [tranthanhtuan@hus.edu.vn](mailto:tranthanhtuan@hus.edu.vn)

*Faculty of Mathematics, Mechanics and Informatics, VNU University of Science, Vietnam, Hanoi, Vietnam*

PHAM CHI VINH: [pcvinh@gmail.com](mailto:pcvinh@gmail.com)

*Faculty of Mathematics, Mechanics and Informatics, VNU University of Science, Vietnam, Hanoi, Vietnam*

GIANG KIEN TRUNG: [trunggk@hus.edu.vn](mailto:trunggk@hus.edu.vn)

*Faculty of Physics, VNU University of Science, Vietnam, Hanoi, Vietnam*

# JOURNAL OF MECHANICS OF MATERIALS AND STRUCTURES

msp.org/jomms

Founded by Charles R. Steele and Marie-Louise Steele

## EDITORIAL BOARD

ADAIR R. AGUIAR	University of São Paulo at São Carlos, Brazil
KATIA BERTOLDI	Harvard University, USA
DAVIDE BIGONI	University of Trento, Italy
MAENGHYO CHO	Seoul National University, Korea
HUILING DUAN	Beijing University
YIBIN FU	Keele University, UK
IWONA JASIUKEWICZ	University of Illinois at Urbana-Champaign, USA
DENNIS KOCHMANN	ETH Zurich
MITSUTOSHI KURODA	Yamagata University, Japan
CHEE W. LIM	City University of Hong Kong
ZISHUN LIU	Xi'an Jiaotong University, China
THOMAS J. PENCE	Michigan State University, USA
GIANNI ROYER-CARFAGNI	Università degli studi di Parma, Italy
DAVID STEIGMANN	University of California at Berkeley, USA
PAUL STEINMANN	Friedrich-Alexander-Universität Erlangen-Nürnberg, Germany
KENJIRO TERADA	Tohoku University, Japan

## ADVISORY BOARD

J. P. CARTER	University of Sydney, Australia
D. H. HODGES	Georgia Institute of Technology, USA
J. HUTCHINSON	Harvard University, USA
D. PAMPLONA	Universidade Católica do Rio de Janeiro, Brazil
M. B. RUBIN	Technion, Haifa, Israel

**PRODUCTION** production@msp.org

SILVIO LEVY Scientific Editor

Cover photo: Ev Shafir

---

See [msp.org/jomms](http://msp.org/jomms) for submission guidelines.

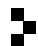
---

JoMMS (ISSN 1559-3959) at Mathematical Sciences Publishers, 798 Evans Hall #6840, c/o University of California, Berkeley, CA 94720-3840, is published in 10 issues a year. The subscription price for 2020 is US \$660/year for the electronic version, and \$830/year (+\$60, if shipping outside the US) for print and electronic. Subscriptions, requests for back issues, and changes of address should be sent to MSP.

---

JoMMS peer-review and production is managed by EditFLOW® from Mathematical Sciences Publishers.

PUBLISHED BY

 **mathematical sciences publishers**  
nonprofit scientific publishing

<http://msp.org/>

© 2020 Mathematical Sciences Publishers

# Journal of Mechanics of Materials and Structures

Volume 15, No. 1

January 2020

---

<b>Stress-minimizing holes with a given surface roughness in a remotely loaded elastic plane</b>	<b>SHMUEL VIGDERGAUZ and ISAAC ELISHAKOFF</b>	<b>1</b>
<b>Analytical modeling and computational analysis on topological properties of 1-D phononic crystals in elastic media</b>	<b>MUHAMMAD and C. W. LIM</b>	<b>15</b>
<b>Dynamics and stability analysis of an axially moving beam in axial flow</b>	<b>YAN HAO, HULIANG DAI, NI QIAO, KUN ZHOU and LIN WANG</b>	<b>37</b>
<b>An approximate formula of first peak frequency of ellipticity of Rayleigh surface waves in an orthotropic layered half-space model</b>	<b>TRUONG THI THUY DUNG, TRAN THANH TUAN, PHAM CHI VINH and GIANG KIEN TRUNG</b>	<b>61</b>
<b>Effect of number of crowns on the crush resistance in open-cell stent design</b>	<b>GIDEON PRAVEEN KUMAR, KEPING ZUO, LI BUAY KOH, CHI WEI ONG, YUCHENG ZHONG, HWA LIANG LEO, PEI HO and FANGSEN CUI</b>	<b>75</b>
<b>A dielectric breakdown model for an interface crack in a piezoelectric bimaterial</b>	<b>YURI LAPUSTA, ALLA SHEVELEVA, FRÉDÉRIC CHAPELLE and VOLODYMYR LOBODA</b>	<b>87</b>
<b>Thermal buckling and free vibration of Timoshenko FG nanobeams based on the higher-order nonlocal strain gradient theory</b>	<b>GORAN JANEVSKI, IVAN PAVLOVIĆ and NIKOLA DESPENIĆ</b>	<b>107</b>
<b>A new analytical approach for solving equations of elasto-hydrodynamics in quasicrystals</b>	<b>VALERY YAKHNO</b>	<b>135</b>
<b>Expansion-contraction behavior of a pressurized porohyperelastic spherical shell due to fluid redistribution in the structure wall</b>	<b>VAHID ZAMANI and THOMAS J. PENCE</b>	<b>159</b>



1559-3959(2020)15:1;1-L